Applied Catalysis B: Environment and Energy 352 (2024) 124055

Contents lists available at ScienceDirect

Applied Catalysis B: Environment and Energy

journal homepage: www.elsevier.com/locate/apcatb

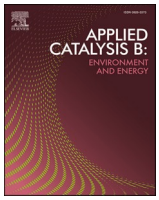

Full valorisation of waste PET into dimethyl terephthalate and cyclic arylboronic esters

Minghao Zhang [a,1], Yunkai Yu [a,1], Binghui Yan [a], Xiuju Song [d], Yu Liu [e], Yixiong Feng [d], Weixiang Wu [a,c], Baoliang Chen [a,c], Buxing Han [b], Qingqing Mei [a,c,*]

[a] Institute of Environment Science and Technology, College of Environmental and Resource Sciences, Zhejiang University, Hangzhou, Zhejiang 310058, China
[b] Institute of Chemistry, Chinese Academy of Sciences, Zhongguancun North First Street 2, Beijing, China
[c] Key Laboratory of Environment Remediation and Ecological Health, Ministry of Education, College of Environmental Resource Sciences, Zhejiang University, Hangzhou 310058, China
[d] School of Mechanical Engineering, Zhejiang University, Hangzhou 310058, China
[e] College of Life Science, Zhejiang University, Hangzhou, Zhejiang 310058, China

ARTICLE INFO

Keywords:
PET methanolysis
Dimethyl terephthalate
Arylboronic esters
Layered double oxides
Waste plastics

ABSTRACT

Developing efficient and cost-effective methodologies for high value-added conversion of waste plastic delivers substantial environmental and economic benefits. Herein, we develop a novel approach utilizing boric acid in the methanolysis of waste polyethylene terephthalate (PET) to derive pure dimethyl terephthalate (DMT) and boronic acid esters through in-situ capture of ethylene glycol (EG). It not only upcycles waste PET but also eliminates intricate EG purification processes. Catalyzed by magnalium-aluminum-layered double oxides (Mg_4Al_1-LDO), this method achieved 100 % conversions of PET with 96 % and 99 % yields of arylboronic esters and DMT, respectively. Kinetic studies and in-situ Fourier-transform infrared spectroscopy (FT-IR) demonstrated the pivotal role of the monodentate methoxy species, generated through the interaction of medium basic Mg–O ion pairs and methanol. This method demonstrates applicability for the upcycling of assorted discarded PET wastes, polyesters, and polycarbonates with EG units, highlighting its potential as a comprehensive solution for waste plastic management.

1. Introduction

Despite the growing awareness of the environmental crisis caused by excessive plastic consumption and inadequate waste management, plastic production continues to rise in tandem with global economic growth [1]. It is predicted that by 2050, the environmental accumulation of plastics could exceed 2.5 billion tons [2]. Polyethylene terephthalate (PET) is one of the most widely used polyester plastics, boasting an annual production of about 70 million tons [2,3]. Unfortunately, only a small fraction of PET waste undergoes recycling, exacerbating the problem as these waste polyester plastics can break down into microplastic pollutants, causing significant ecological damage [4,5]. Therefore, developing efficient technologies to convert waste PET carbon resources into value-added commodities has significant environmental and economic benefits. Current PET disposal methods include thermal, mechanical, and chemical recycling [6–8]. Chemical recycling allows for the transformation of polymer to original monomer, fuel, or other high-value products, thereby amplifying the value chain and product quality [6,9].

PET can be chemically depolymerized by nucleophilic agents to cleave the ester group towards monomers or their derivatives [7,10–14]. Hydrolysis and alcoholysis are the most widely used methods to recycle monomers for new PET syntheses [15–17], and extensive studies are carried out to improve the efficiency and reduce the cost [18–23]. Parallel to this closed-loop recycling, a more promising strategy is to make use of the structural characteristics of waste PET as feedstock for more valuable chemicals. Highly selectively transforming the original building blocks is the key to effective construction of target high-value products. For example, by catalytically hydrogenating the ester group directly or after solvolysis, a range of value-added chemicals could be produced, including alcohols [15,24], aromatics [10,16,25], and carboxylic acid derivatives [12]. However, keeping TPA or DMT units is

* Correspondence to: 866 Yuhangtang Road, Hangzhou 310058, China.
E-mail address: meiqq@zju.edu.cn (Q. Mei).
[1] These authors contributed equally.

https://doi.org/10.1016/j.apcatb.2024.124055
Received 24 January 2024; Received in revised form 24 March 2024; Accepted 6 April 2024
Available online 7 April 2024

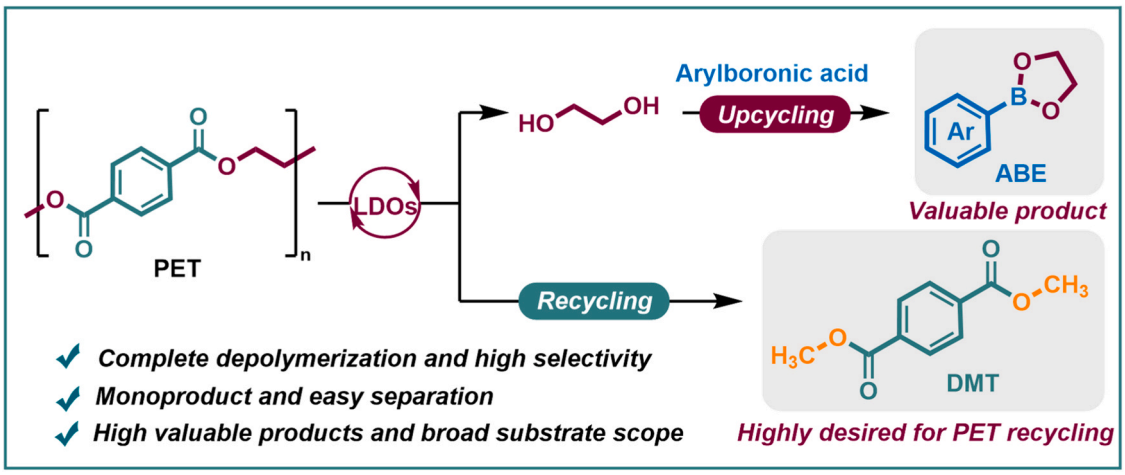

Scheme 1. Waste PET upcycling by in situ capturing EG with arylboronic acid in the methanolysis process.

still highly desired due to their great market demand as PET and PBAT (polybutylene adipate terephthalate, a biodegradable plastic) monomers. In addition, the high boiling point and strong hydrogen-bonding capacity of ethylene glycol (EG) escalate the energy consumption of purification, especially in aqueous systems. This necessitates exploring methods to upgrade EG into more valuable chemicals, thereby preserving high-value TPA/DMT while bypassing the arduous purification of EG. The most widely reported approaches are partial oxidation of EG into formic acid or its salts [17,26–29]. Despite these promising achievements, more valuable and facile routes to upgrade waste PET towards diverse value-added products based on its building units are yet to be developed.

Herein, we pioneer a facile EG upcycling strategy coupled with PET methanolysis, enabling the synthesis of diverse five-membered

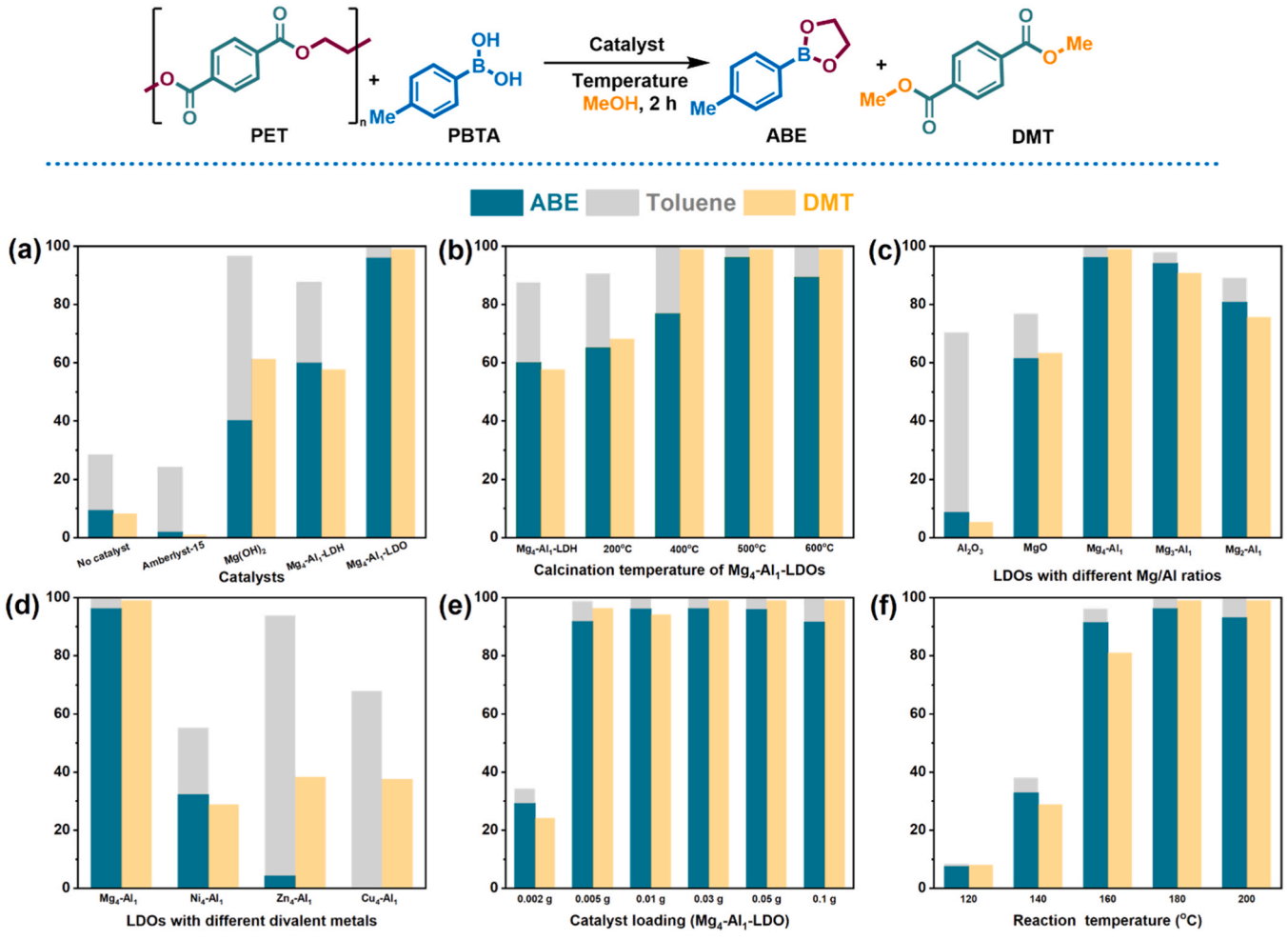

Fig. 1. Catalytic system and reaction condition exploration. Standard reaction conditions: PET (1 mmol), PTBA (1 mmol), catalyst (0.03 g), and MeOH (5 mL) at 180°C for 2 h.

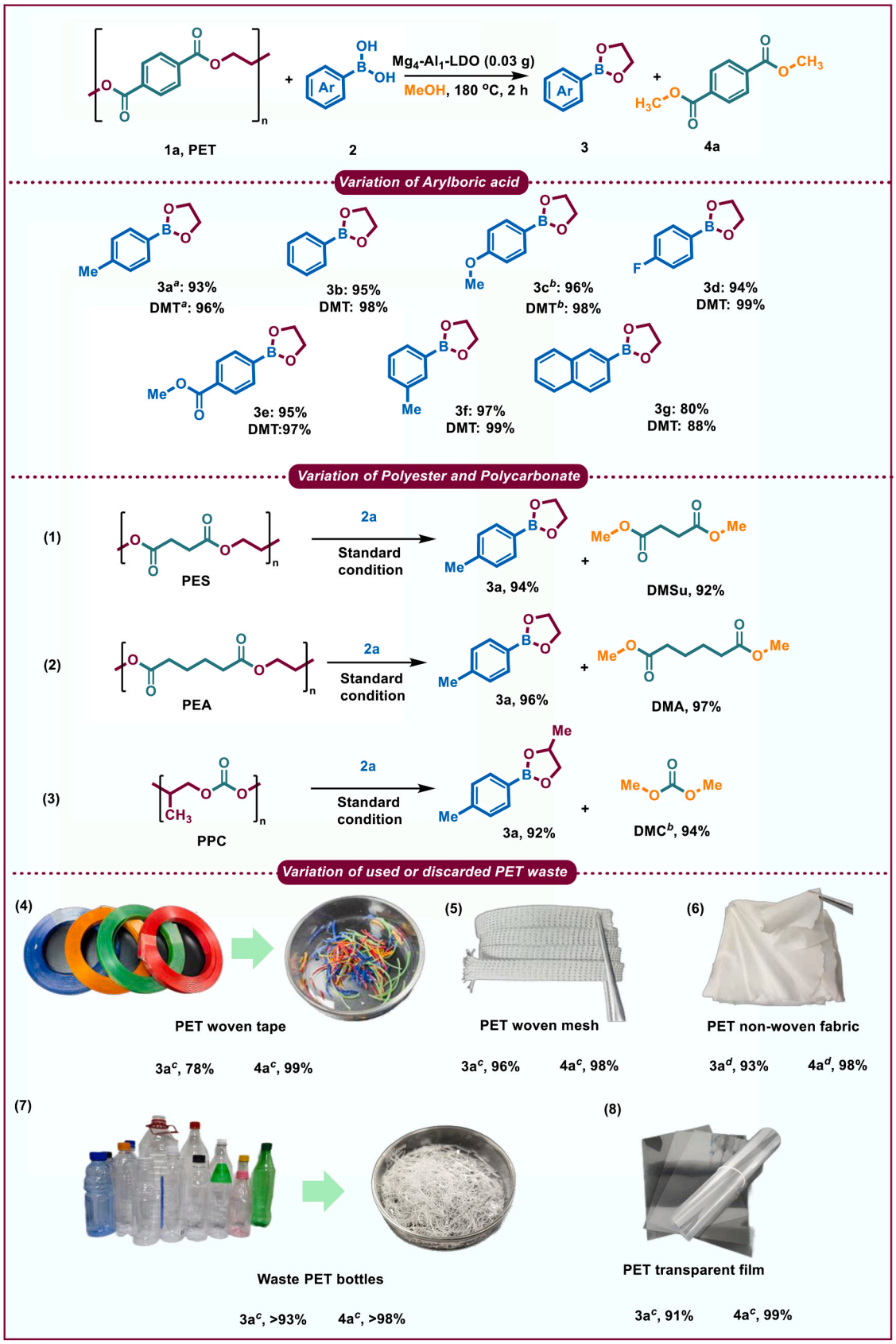

Fig. 2. Scope of substrates. Waste polyester plastics were simply cut into tiny shapes before participating in the reaction. Standard reaction conditions: polyester (1 mmol), boric acid (1 mmol), Mg_4-Al_1-LDO (0.03 g), and MeOH (5 mL) at 180°C for 2 h. [a]PET (5 mmol). [b]yield was given by ^{1}H NMR. [c]at 180°C for 3 h. [d]at 180°C for 4 h.

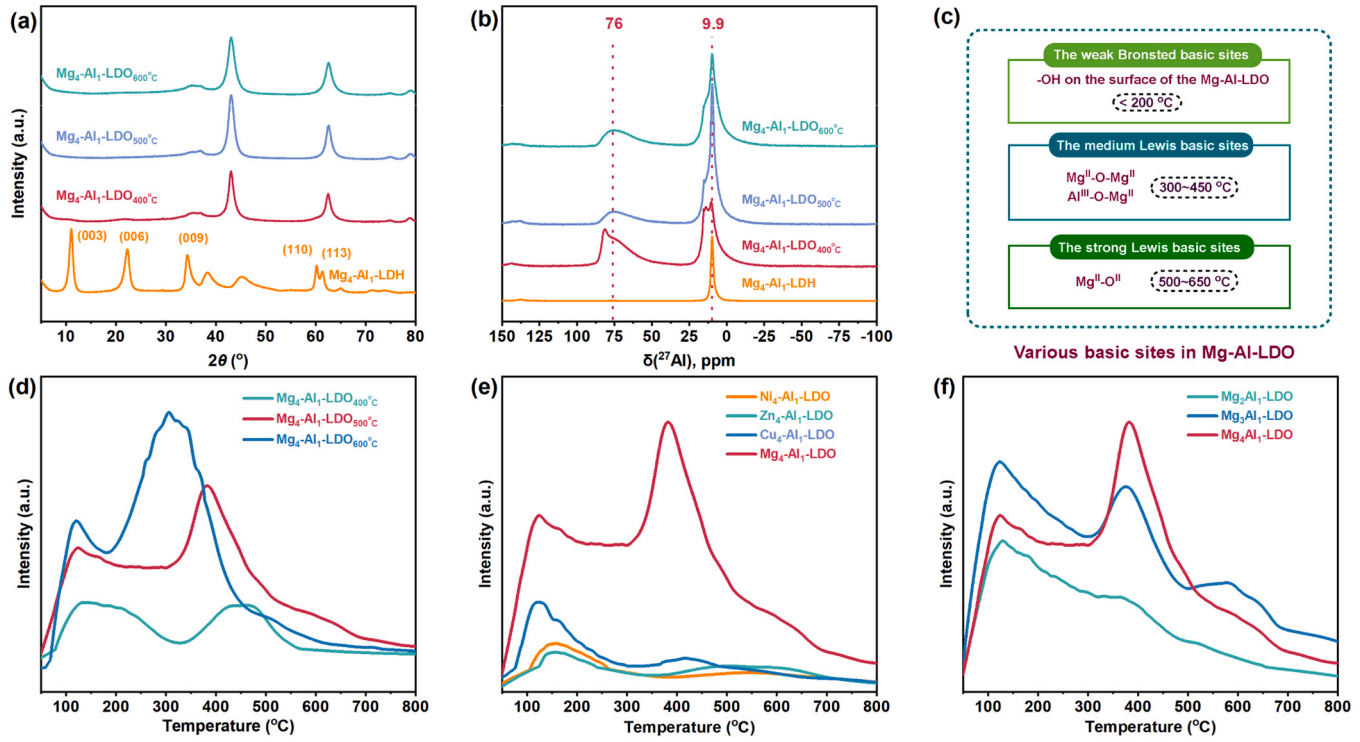

Fig. 3. XRD pattern and CO_2-TPD spectra of various catalysts. (a) XRD patterns of Mg_4-Al_1-LDH and LDOs with different calcination temperature; (b) ^{27}Al MAS NMR spectra of Mg_4-Al_1-LDH and LDOs with different calcination temperature; (c) Typical basic sites of LDOs and the corresponding temperature range in CO_2-TPD; (d) CO_2-TPD of Mg_4-Al_1-LDOs with different calcination temperatures; (e) CO_2-TPD of LDOs with different bivalent metals; (f) CO_2-TPD of Mg-Al-LDOs with different Mg/Al ratios.

arylboronic esters (ABE) and DMT (Scheme 1). Arylboronic esters are important organic boron compounds widely used in coupling reactions for the efficient construction of pharmaceuticals and natural products [30–34]. They are typically obtained by reversible binding of diols and boric acid. In this work, by simply introducing arylboric acid into the methanolysis system of waste PET, the reaction can proceed completely and the utilization value of EG is significantly improved by upgrading to valuable arylboronic esters. The process, facilitated by basic layered double oxides (LDOs), successfully achieved 100 % conversions of PET and boric acid with 96 % and 99 % production yields of arylboronic esters and DMT, respectively. The precipitated DMT crystals can be easily separated and purified by recrystallization as high-quality monomer for new PET; the dissolved boronic acid esters can be easily purified through evaporative crystallization for further use in organic synthesis. Overall, this work paves a new way for effective recycling of waste polyester plastics, owing to its advantages such as complete utilization and high selectivity, easy separation and purification, and highly valuable products with broad substrate scope.

2. Results and discussion

2.1. Catalytic system exploration

The devised methodology for waste PET upcycling involves PET methanolysis into DMT+EG and EG capture via esterification with arylboric acid to afford ABE. The initial experiment conducted without a catalyst resulted in limited depolymerization of PET waste, with only 8 % DMT and 10 % ABE yield after operating at 180°C for two hours. Meanwhile, the toluene byproduct was generated undesirably with the yield of 19 %, which was attributed to the rapid protodeboronation of arylboric acid (Ar-B → Ar-H) with the assistance of water [35,36]. As acid or base can catalyze both methanolysis and esterification reactions, some typical acids and bases were tested and yields of DMT and ABE heavily depended on the catalyst used. Fig. 1a demonstrated that acidic Amberlyst-15 exhibited negligible promotion towards PET methanolysis, resulting in almost unchanged DMT and ABE yields. Conversely, basic $Mg(OH)_2$ and magnesium-aluminum layered double hydroxides (Mg-Al-LDHs) enhanced the production of DMT and ABE. Notably, under identical conditions (180°C, 2 h), Mg_4-Al_1-LDH achieved remarkable yields of 60 % for ABE, 58 % for DMT, along with a toluene byproduct yield of 28 %. However, incomplete PET depolymerization and undesired protodeboronation of *p*-tolylboronic acid into toluene were still observed. This issue is likely due to the inadequate basicity of Mg-Al-LDH and the presence of copious interlayer water molecules and hydroxide ions. Previous studies have confirmed that the expulsion of interlayer water molecules and hydroxide ions from LDHs by high-temperature calcination results in the formation of layered double oxides (LDOs) with stronger basicity [37,38]. Thus, we synthesized Mg_4-Al_1-LDOs with various calcination temperatures to mitigate the effects of water and hydroxide ions in hydrotalcite layers. As anticipated, calcination significantly improved ABE and DMT yields, and increasing calcination temperatures proved favorable for PET depolymerization (Fig. 1b). When the calcination temperature was 500°C, the yield of ABE and DMT reached 96 % and 99 %, respectively, effectively suppressing the protodeboronation of *p*-tolylboronic acid. In comparison, commercially available acidic Al_2O_3 and basic MgO were used as catalysts for the PET methanolysis. The results demonstrate that Al_2O_3 exhibits negligible catalytic activity for PET methanolysis. suggesting that the acidity of Al_2O_3 is insufficient to catalyze PET methanolysis effectively. On the other hand, MgO promotes the depolymerization of PET, resulting in the formation of ABE and DMT with yields of 61 % and 63 %, respectively. However, these yields are lower compared to those achieved using Mg-Al-LDOs. These findings indicate that the Lewis acid-base pairs present in Mg-Al-LDOs are crucial for the adsorption of methanol and the deprotonation process during PET depolymerization. These Lewis acid-base pairs play an indispensable role in facilitating the

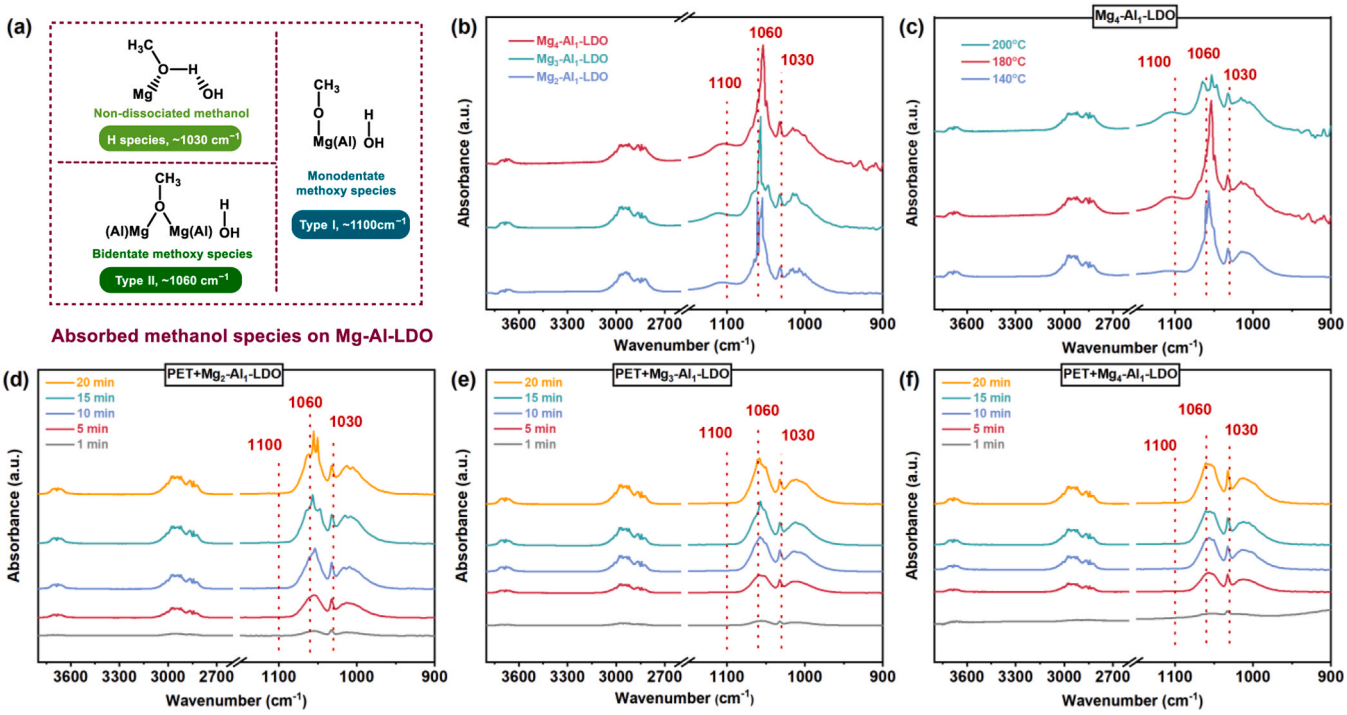

Fig. 4. (a) Possible adsorbed methanol species on Mg-Al-LDO and the corresponding IR characteristic peak positions; IR spectra of methanol adsorption over different Mg-Al-LDO catalysts: (b) Mg-Al-LDOs with different Mg/Al ratio; (c) Mg_4-Al_1-LDO with different adsorption temperatures; (d-f) Mg-Al-LDO (d: Mg_2-Al_1-LDO, e: Mg_3-Al_1-LDO, f: Mg_4-Al_1-LDO) with PET during different adsorption time at 180°C.

PET methanolysis reaction [39]. The influence of the Mg/Al molar ratio in Mg-Al-LDOs was also investigated (Fig. 1c). A lower Mg/Al ratio resulted in weakened PET depolymerization and reduced yields of ABE and DMT. LDOs containing different divalent metals (Ni^{2+}, Zn^{2+}, and Cu^{2+}) were tested as well, but these alternatives resulted in lower ABE and DMT yields (Fig. 1d), due to their weaker basicity [40–42]. Furthermore, we examined the effect of catalyst loading. Incomplete PET depolymerization occurred when an insufficient amount of catalyst was used (Fig. 1e). Increasing catalyst loading proved beneficial for both PET methanolysis and arylboric acid esterification. With a catalyst loading of 0.03 g, both PET and *p*-tolylboronic acid were entirely converted into ABE and DMT, yielding 96 % and 99 %, respectively, at 180°C for 2 h (Fig. 1e). Further increase in the amount of LDOs to 0.1 g does not affect the methanolysis, but slightly reduces the yield of ABE due to the enhanced protodeboronation of arylboric acid. In contrast, systematically decreasing the catalyst loading to 0.002 g significantly constrains PET depolymerization, ultimately yielding 30 % ABE and 24 % DMT. Adjusting the reaction temperature resulted in lower ABE yields (Fig. 1f). Operating the Mg_4-Al_1-LDO at a lower temperature of 140°C only yielded 33 % ABE and 29 % DMT for 2 h (Fig. 1f). In contrast, an elevated temperature of 200°C promoted protodeboronation of *p*-tolylboronic acid to produce toluene side product (Fig. 1f). Moreover, when scaling up the reaction five times under optimal condition, we also achieved high yields of the five-membered cyclic product ABE (93 %, **3a** in Fig. 2). Catalyst recycling test demonstrated that Mg_4-Al_1-LDO can be reused for 5 times without significant deactivation, and the peak performance of the catalyst can be simply regained by calcination (Fig. S2 and Fig. S3).

Subsequently, we tested the compatibility of the system with various arylboronic acids. Encouragingly, the system accommodated arylboronic acids bearing different functional groups on the benzene ring, affording various five-membered annulation arylboronic esters **3b-3f** in 95–97 % yield and DMT in 97–99 % yield (Fig. 2). The system demonstrated excellent tolerance of the electronic properties of arylboronic acids, regardless containing electron-donating (-OMe) or electron-withdrawing groups (-F, -CO_2Me), or the position of the substituent on the benzene ring (-*m*-Me). Furthermore, 1-naphthylboric acid also displayed high reactivity and successfully reacted with PET to provide the cyclic product **3 g** in a satisfactory yield (80 %). Intriguingly, other waste plastics with adjacent diol units, such as poly(ethylene succinate) (PES) and poly(ethylene adipate) (PEA), and polycarbonates like poly (propylene carbonate) (PPC), which are widely used across various fields, were viable candidates for our process. They can be converted into corresponding borate esters and diesters with impressive yields (Fig. 2, Nos. 1–3) under standard conditions. To further validate the practicality of this new method, we tested varieties of waste commercial PET samples, including woven tape, woven mesh, transparent film, and non-woven fabric. Excitingly, ABE and DMT were harvested with high yields (Fig. 2, Nos. 4–6, 8). Moreover, this catalytic system can also be effectively applied in the upcycling of twelve different waste PET bottles. All tests demonstrated high yields of both ABE and DMT, regardless of previous use or disposal status of the bottles (Fig. 2, No. 7, and Table S1 for detailed data).

2.2. Characterization of catalysts

X-ray diffraction (XRD) experiments were performed to confirm the structure of the catalysts and the patterns are shown in Fig. 3a. Strong (003), (006), (009), (110), (113) and broadened (015), (018) reflections were observed for the Mg_4-Al_1-LDH sample (Fig. 3a), which are the characteristic diffraction peaks of hydrotalcite-like compounds [39]. Upon calcination at high temperatures (400, 500, and 600°C), the hydrotalcite-like solids undergo decarbonation and dehydration processes, forming mixed metal oxides (Mg_4-Al_1-LDO). All the calcinated Mg_4-Al_1-LDOs exhibit the peaks similar to periclase MgO, characterized by the peaks at 43° and 63° with no residual traces of the hydrotalcite phase [37,39]. No phases containing aluminum were detected, indicating that Al^{3+} is highly dispersed in a mixed oxide phase. This result shows that the hydrotalcite-like structure of Mg_4-Al_1-LDH has been fully converted into the mixed oxide phase of Mg_4-Al_1-LDO by destroying the

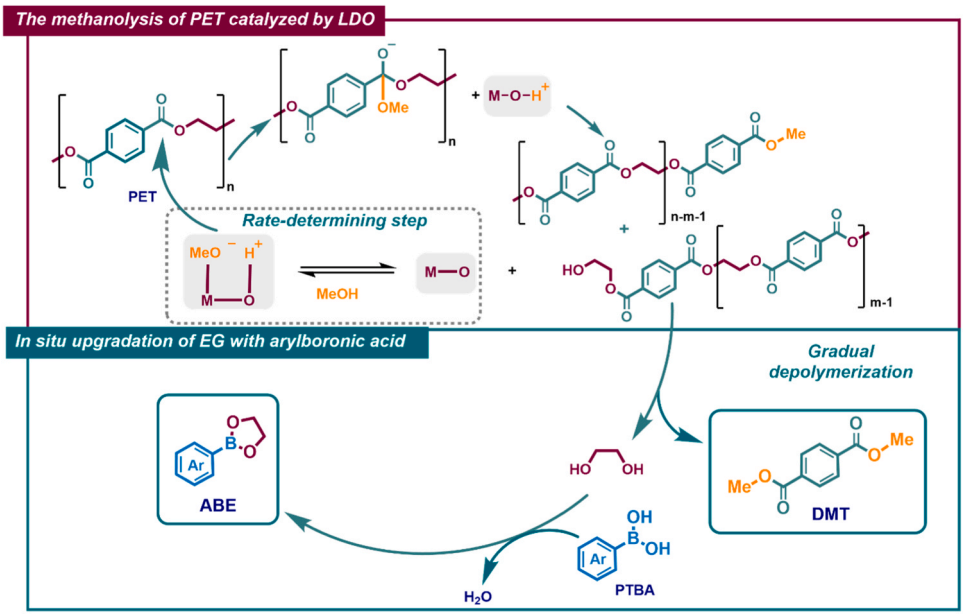

Fig. 5. The possible reaction mechanism of PET methanolysis coupled with in situ EG upgradation into cyclic arylboronic esters over Mg-Al-LDO.

layered structure under high temperature (400–600°C). In order to obtain a more in-depth understanding of the structural changes that occur during calcination, ^{27}Al MAS NMR analysis was performed. Fig. 3b shows the ^{27}Al MAS NMR spectra of Mg_4-Al_1-LDH and Mg_4-Al_1-LDO calcined at different temperatures ranging from 400 to 600°C. As anticipated, the spectrum of fresh Mg_4-Al_1-LDH exhibited a single resonance near 9.9 ppm, which can be assigned to octahedrally coordinated Al [43]. This data confirmed that the LDH structure is formed by metals coordinated to six hydroxyl groups with octahedral geometry. However, when the samples were calcined at 400°C, a new signal at around 80 ppm was observed. Meanwhile, the six-coordinated Al resonance is quite broad and shifts slightly to 13 ppm. These can be attributed to the formation of tetrahedrally coordinated Al. This suggests that after calcination, the Al coordination partially changes from six-coordinated to four-coordinated due to the removal of CO_3^{2-} and H_2O. By further increasing the calcination temperature to 500 or 600°C, the resonance of six-coordinated Al shifts towards 15 ppm. Simultaneously, the relative intensity of the tetrahedrally coordinated Al resonance becomes broader and weaker, and shifts to 76 ppm. These changes indicate the presence of more distorted environments in the mixed oxide phase of Mg_4-Al_1-LDO [44]. Therefore, the calcination process leads to the transformation of the hydrotalcite structure into a mixed oxide phase, a phenomenon further corroborated by the data derived from the characterization results from nitrogen adsorption (Table S2) and SEM images (Fig. S5).

As the catalytic activity heavily depends on the basicity of the catalysts, we employed temperature-programmed desorption of CO_2 (CO_2-TPD) to characterize the basicity property. Based on previous literature, we can categorize CO_2 desorption temperatures (T_d) below 200°C as weak Brönsted basic sites [45]. Therefore, it is crucial to carefully consider the impact of calcination on the catalytic properties. All Mg_4-Al_1-LDOs with varying calcination temperatures predominantly exhibit weak and medium basic sites, as indicated in Fig. 3d. With a calcination temperature at 400°C, Mg_4-Al_1-$LDO_{400°C}$ produces ABE and DMT with 77 % and 99 % yield, respectively, along with a 23 % yield of toluene, outperforming Mg_4-Al_1-LDH due to the eradication of Brönsted OH^- basic sites (Fig. 1b). Raising the calcination temperature from 400°C to 600°C, the CO_2 adsorption peaks shift to lower temperatures with increased base capacity (Fig. 3d). As a result, the reaction selectivity using Mg_4-Al_1-$LDO_{500°C}$ were improved, with 4 % yield of protodeboronation product (Fig. 1b). However, when the calcination temperature was raised to 600°C, Mg_4-Al_1-$LDO_{600°C}$ exhibited an excessive amount of basicity, which resulted in a higher yield of protodeboronation product toluene (11 %). To further understand the influence of basic strength on the catalytic activity, LDOs with different metals were prepared (Fig. S4b). Fig. 3e shows that the Ni_4-Al_1-LDO, Zn_4-Al_1-LDO, and Cu_4-Al_1-LDO catalysts have significantly less basicity compared to the Mg-Al-LDOs. These LDOs mainly contain weak basic sites with negligible medium and strong basic sites. They exhibited underwhelming ABE and DMT yields, even comparable to the catalyst-free condition. We posit that weak basic sites may lack the ability to catalyze PET depolymerization effectively[37,39]. This suggests that medium basic Mg–O ion pairs are the actual active sites. To verify this, Mg-Al-LDO with different Mg/Al molar ratios were studied (Fig. 3f and Fig. S4a). As the Mg/Al ratio increases from 2 to 4, the peak area of medium basic sites versus weak basic sites also increases. Mg_2-Al_1-LDO mainly has weak basic sites and yields 81 % ABE and 76 % DMT (Fig. 1c). Mg_3-Al_1-LDO has considerable medium basic sites but is still dominated by weak basic sites, resulting in increased ABE and DMT yields of 94 % and 91 %, respectively (Fig. 1c). Mg_4-Al_1-LDO possesses more medium basic sites, leading to 96 % and 99 % yields of ABE and DMT (Fig. 1c) respectively. To further quantify the impact of alkalinity on the reaction activity, we performed a deconvolution of the CO_2-TPD results. The results indicate that with the increase in the content of medium-basic Mg–O ion pairs, the reaction activity correspondingly increases (Fig. S6 and Table S3). These results highlight the critical role of medium basic Mg–O ion pairs in the LDOs for both the reaction activity and selectivity.

2.3. Reaction mechanism

As previously discussed, medium basic Mg–O ion pairs play a crucial role in PET depolymerization. Reaction kinetics studies demonstrates that methanolysis of PET is the rate-determining step in this system (Fig. S7). To shed light on the rate-determining methanolysis step and get insight into the reaction mechanism, we conducted in situ IR spectroscopy analysis. The depicted spectra signify the difference IR spectra with the pre-heated sample serving as the reference point. Methanol adsorption on Mg-Al-LDO at various temperatures (Fig. 4b) with different Mg/Al ratios (Fig. 4c) was studied. The interaction between methanol and the catalyst surfaces induces changes in two primary regions, 3100 ~ 2700 cm^{-1} and 1200 ~ 1000 cm^{-1}, which corresponds to

the $\nu(CH_3)$ and ν(O-C) vibration mode of methanol and/or methoxy species, respectively. Post-methanol adsorption IR spectra of LDOs reveal the formation of three types of active adsorbed species, each with distinct (O-C) vibrations. These include non-dissociated methanol (H species, ~1030 cm^{-1}), monodentate methoxy species (Type I, ~1100 cm^{-1}) and bidentate methoxy species (Type II, ~1060 cm^{-1}) [39,46], as shown in Fig. 4a.

Upon introduction of methanol via argon bubbling, three types of intermediates emerge, with bidentate species Type II at 1060 cm^{-1} and non-dissociated methanol at 1030 cm^{-1} dominating, and a weak band for monodentate species Type I at 1100 cm^{-1}. As the methanol adsorption time increases, the band area of all intermediate species increases, suggesting an enhanced interaction between the Mg–O active site and methanol (Fig. S8). After 15 min of methanol adsorption, the band areas of the adsorbed methanol stopped increasing, indicating saturation of methanol adsorption. To investigate the relationship between the infrared spectra of Mg-Al-LDO with different Mg/Al ratios and the PET depolymerization activity, we compared the infrared spectra of Mg-Al-LDO with adsorbed methanol at saturation (20 min) at 180°C. As shown in Fig. 4b, the band areas of Type II and H species intermediates were comparable, while Type I showed significant differences, which increased with the Mg/Al ratio and correlated with the order of PET depolymerization activity (Fig. 1c). This suggests that Type I plays a crucial role in the reaction, as it has been reported to be the active intermediate in the methanol transesterification reaction [39]. And based on the previous studies, H species does not seem to be related with transesterification reaction due to its lability, whereas the structural stability of the Type II species is not favourable to providing rich active sites [39]. Conversely, Type I species play a pivotal role by enabling nucleophilic attacks on the carbon atom within the ester group of PET, a capability underscored by strong basicity as evidenced by CO_2-TPD results (Fig. 3, Fig. S6 and Table S3). We then compared the infrared spectra of Mg_4-Al_1-LDO with adsorbed methanol at saturation (20 min) at different temperatures (140°C, 180°C, and 200°C). Similarly, the band area of Type II and H species intermediates were comparable, while Type I displayed a distinctly different band area that increased with temperature (Fig. 4c). More Type I species favored the methanolysis of PET at 200°C than at 180°C, but excessive temperatures easily induced the undesirable protodeboronation of arylboric acid (Fig. 1f). To further verify the relationship between Type I adsorption mode and reaction activity, Table S2 outlines the deconvoluted band area for LDOs with different Mg/Al ratios and temperatures, normalized by catalyst weight [37,39]. The results show that DMT yield is positively associated with methoxy Type I area, suggesting a direct link between Type I methoxy species and PET methanolysis. To further explore the function of Type I monodentate species in the PET methanolysis process, we analyzed the reaction with in-situ IR spectroscopy by introducing PET as a reactant. Mg-Al-LDO with different Mg/Al ratios were mixed with PET in a 3:1 mass ratio. Notably, for all catalysts at 180°C, the presence of PET results in complete disappearance of the band at 1100 cm^{-1} after methanol adsorption, while the other methoxy bands remained almost unaltered (Fig. 4d-f). This observation confirms that methoxy Type I can react rapidly with PET, emphasizing its crucial role in the reaction.

Building upon reported work [47] and our current experimental findings, we propose a plausible mechanism for this chemical upcycling process, as depicted in Fig. 5. Initially, Mg–O in Mg-Al-LDO activates methanol by extracting its protons, forming CH_3O^-. This CH_3O^- intermediate then functions as a nucleophilic reagent, attacking the C═O of PET and leading to a tetrahedral intermediate, which gradually breaks down the long chain to generate DMT and EG, facilitated by H^+ on the surface of the LDOs. As the molecular chain shortens and molecular weight reduces, DMT, PET oligomers, and EG fragments are generated due to efficient cleavage of the ester C═O bond. The oligomers then rapidly decompose, leading to an increased yield of DMT and EG fragments. Concurrently, the in-situ produced EG is swiftly captured by arylboric acid, aided by Mg_4-Al_1-LDO, during the methanolysis process. This sequence leads to a dehydration cyclic reaction, yielding ABE product.

3. Conclusion

In this study, we have proposed an effective and facile method for the upcycling of waste PET to afford various value-added five-membered cyclic arylboronic esters and dimethyl terephthalate (DMT) in optimal yields. Facilitated by the Mg_4-Al_1-LDO catalyst, the reaction demonstrates a complete conversion of PET and boric acid, yielding 96 % and 99 % of arylboronic esters and DMT, respectively. Kinetic study reveals that the rate-determining step in this entire process is the methanolysis of PET. In-situ Fourier-transform infrared spectroscopy (FT-IR) demonstrates that methanol adsorbed on the medium basic Mg–O ion pairs, and the resulted monodentate methoxy species plays a pivotal role in the catalytic process. The catalyst can be recycled and easily regenerated. This method can be successfully extended to recycle various types of waste PET, offering a pragmatic solution for high-value chemical recycling of plastic waste. It could potentially mark a significant step in addressing the global plastic waste challenge and pave a new way for more efficient and environmentally friendly recycling methods.

CRediT authorship contribution statement

Buxing Han: Resources, Writing – review & editing. **Qingqing Mei:** Writing – review & editing, Supervision, Resources, Funding acquisition, Formal analysis, Conceptualization. **Minghao Zhang:** Writing – original draft, Investigation, Formal analysis, Data curation. **Yunkai Yu:** Writing – original draft, Investigation, Formal analysis, Data curation. **Binghui Yan:** Formal analysis. **Xiuju Song:** Formal analysis, Resources. **Yu Liu:** Data curation. **Yixiong Feng:** Writing – review & editing. **Weixiang Wu:** Formal analysis. **Baoliang Chen:** Writing – review & editing.

Declaration of Competing Interest

We declare that we do not have any commercial or associative interest that represents a conflict of interest in connection with the work submitted.

Data availability

No data was used for the research described in the article.

Acknowledgement

This work was supported by National Natural Science Foundation of China (22209146, 22376183, 22293015), the Fundamental Research Funds for the Zhejiang Provincial Universities (226-2023-00041), the Fundamental Research Funds for the Central Universities (226-2023-00077), and Key Research and Development Program of Zhejiang Province (2024C03112).

Appendix A. Supporting information

Supplementary data associated with this article can be found in the online version at doi:10.1016/j.apcatb.2024.124055.

References

[1] M. MacLeo, H.P.H. Arp, M.B. Tekman, A. Jahnke, The global threat from plastic pollution, Science 373 (2021) 61–65.
[2] R. Geyer, J.R. Jambeck, K.L. Law, Production, use, and fate of all plastics ever made, Sci. Adv. 3 (2017) 5.
[3] X.Y. Wu, M.V. Galkin, T. Stern, Z.H. Sun, K. Barta, Fully lignocellulose-based PET analogues for the circular economy, Nat. Commun. 13 (2022) 12.

[4] M.E. Seeley, B. Song, R. Passie, R.C. Hale, Microplastics affect sedimentary microbial communities and nitrogen cycling, Nat. Commun. 11 (2020) 10.
[5] M.C. Rillig, A. Lehmann, Microplastic in terrestrial ecosystems, Science 368 (2020) 1430–1431.
[6] A.J. Martín, C. Mondelli, S.D. Jaydev, J. Pérez-Ramírez, Catalytic processing of plastic waste on the rise, Chem 7 (2021) 1487–1533.
[7] M.Y. Chu, Y. Liu, X.X. Lou, Q. Zhang, J.X. Chen, Rational design of chemical catalysis for plastic recycling, ACS Catal. 12 (2022) 4659–4679.
[8] Y. Peng, J. Yang, C. Deng, J. Deng, L. Shen, Y. Fu, Acetolysis of waste polyethylene terephthalate for upcycling and life-cycle assessment study, Nat. Commun. 14 (2023) 3249.
[9] K.S. Hu, Y.Y. Yang, Y.X. Wang, X.G. Duan, S.B. Wang, Catalytic carbon and hydrogen cycles in plastics chemistry, Chem. Catal. 2 (2022) 724–761.
[10] Z.W. Gao, B. Ma, S. Chen, J.Q. Tian, C. Zhao, Converting waste PET plastics into automobile fuels and antifreeze components, Nat. Commun. 13 (2022) 9.
[11] D.D. Pham, J. Cho, Low-energy catalytic methanolysis of poly (ethyleneterephthalate), Green. Chem. 23 (2021) 511–525.
[12] Y.W. Li, M. Wang, X.W. Liu, C.Q. Hu, D.Q. Xiao, D. Ma, Catalytic Transformation of PET and CO_2 into High-Value Chemicals, Angew. Chem. Int. Ed. 61 (2022) 5.
[13] E. Barnard, J.J.R. Arias, W. Thielemans, Chemolytic depolymerisation of PET: a review, Green Chem. 23 (2021) 3765–3789.
[14] S.B. Zhang, Y.Y. Xue, Y.F. Wu, Y.X. Zhang, T. Tan, Z.Q. Niu, PET recycling under mild conditions via substituent-modulated intramolecular hydrolysis, Chem. Sci. 14 (2023) 6558–6563.
[15] S. Westhues, J. Idel, J. Klankermayer, Molecular catalyst systems as key enablers for tailored polyesters and polycarbonate recycling concepts, Sci. Adv. 4 (2018) 8.
[16] Y.X. Jing, Y.Q. Wang, S.Y. Furukawa, J. Xia, C.Y. Sun, M.J. Hulsey, H.F. Wang, Y. Guo, X.H. Liu, N. Yan, Towards the circular economy: converting aromatic plastic waste back to arenes over a Ru/Nb_2O_5 catalyst, Angew. Chem. Int. Ed. 60 (2021) 5527–5535.
[17] H. Zhou, Y. Ren, Z.H. Li, M. Xu, Y. Wang, R.X. Ge, X.G. Kong, L.R. Zheng, H. H. Duan, Electrocatalytic upcycling of polyethylene terephthalate to commodity chemicals and H_2 fuel, Nat. Commun. 12 (2021) 9.
[18] R. Lopez-Fonseca, I. Duque-Ingunza, B. de Rivas, L. Flores-Giraldo, J.I. Gutierrez-Ortiz, Kinetics of catalytic glycolysis of PET wastes with sodium carbonate, Chem. Eng. J. 168 (2011) 312–320.
[19] W.S. Yang, J. Wang, L. Jiao, Y. Song, C. Li, C.Q. Hu, Easily recoverable and reusable p-toluenesulfonic acid for faster hydrolysis of waste polyethylene terephthalate, Green. Chem. 24 (2022) 1362–1372.
[20] Y.C. Liu, X.Q. Yao, H.Y. Yao, Q. Zhou, J.Y. Xin, X.M. Lu, S.J. Zhang, Degradation of poly(ethylene terephthalate) catalyzed by metal-free choline-based ionic liquids, Green. Chem. 22 (2020) 3122–3131.
[21] M.J. Kang, H.J. Yu, J. Jegal, H.S. Kim, H.G. Cha, Depolymerization of PET into terephthalic acid in neutral media catalyzed by the ZSM-5 acidic catalyst, Chem. Eng. J. 398 (2020) 9.
[22] A.V. Pinto, P. Ferreira, R.P.P. Neves, P.A. Fernandes, M.J. Ramos, A.L. Magalhaes, Reaction mechanism of MHETase, a PET degrading Enzyme, ACS Catal. 11 (2021) 10416–10428.
[23] G.J. Palm, L. Reisky, D. Böttcher, H. Müller, E.A.P. Michels, M.C. Walczak, L. Berndt, M.S. Weiss, U.T. Bornscheuer, G. Weber, Structure of the plastic-degrading Ideonella sakaiensis MHETase bound to a substrate, Nat. Commun. 10 (2019) 10.
[24] C.Y. Wang, O. El-Sepelgy, Reductive depolymerization of plastics catalyzed with transition metal complexes, Curr. Opin. Green. Sustain. Chem. 32 (2021) 6.
[25] M.X. Ye, Y.R. Li, Z.R. Yang, C. Yao, W.X. Sun, X.X. Zhang, W.Y. Chen, G. Qian, X. Z. Duan, Y.Q. Cao, L.A. Li, X.G. Zhou, J. Zhang, Ruthenium/TiO_2-catalyzed hydrogenolysis of polyethylene terephthalate: reaction pathways dominated by coordination environment, Angew. Chem. Int. Ed. 62 (2023) e202301024.
[26] X. Li, J.Y. Wang, T. Zhang, T.F. Wang, Y.X. Zhao, Photoelectrochemical catalysis of waste polyethylene terephthalate plastic to coproduce formic acid and hydrogen, ACS Sustain. Chem. Eng. 10 (2022) 9546–9552.
[27] F.L. Liu, X.T. Gao, R. Shi, E.C.M. Tse, Y. Chen, A general electrochemical strategy for upcycling polyester plastics into added-value chemicals by a $CuCo_2O_4$ catalyst, Green. Chem. 24 (2022) 6571–6577.
[28] J.Y. Wang, X. Li, T. Zhang, Y.T. Chen, T.F. Wang, Y.X. Zhao, Electro-reforming polyethylene terephthalate plastic to co-produce valued chemicals and green hydrogen, J. Phys. Chem. Lett. 13 (2022) 622–627.
[29] J.Y. Wang, X. Li, M.L. Wang, T. Zhang, X.Y. Chai, J.L. Lu, T.F. Wang, Y.X. Zhao, D. Ma, Electrocatalytic valorization of poly(ethylene terephthalate) plasticand CO_2 for simultaneous production of formic acid, ACS Catal. 12 (2022) 6722–6728.
[30] Y. Iwai, K.M. Gligorich, M.S. Sigman, Aerobic alcohol oxidation coupled to palladium-catalyzed alkene hydroarylation with boronic esters, Angew. Chem. Int. Ed. 47 (2008) 3219–3222.
[31] G. Ranjani, R. Nagarajan, Insight into copper catalysis: in situ formed nano Cu_2O in Suzuki-Miyaura cross-coupling of aryl/indolyl boronates, Org. Lett. 19 (2017) 3974–3977.
[32] R.H. Li, Z.C. Ding, C.Y. Li, J.J. Chen, Y.B. Zhou, X.M. An, Y.J. Ding, Z.P. Zhan, Thiophene-alkyne-based CMPs as highly selective regulators for oxidative heck reaction, Org. Lett. 19 (2017) 4432–4435.
[33] Y.B. Zhou, Y.Q. Wang, L.C. Ning, Z.C. Ding, W.L. Wang, C.K. Ding, R.H. Li, J. J. Chen, X. Lu, Y.J. Ding, Z.P. Zhan, Conjugated microporous polymer as heterogeneous ligand for highly selective oxidative Heck reaction, J. Am. Chem. Soc. 139 (2017) 3966–3969.
[34] N. Yasuda, Application of cross-coupling reactions in Merck, J. Organomet. Chem. 653 (2002) 279–287.
[35] P.A. Cox, M. Reid, A.G. Leach, A.D. Campbell, E.J. King, G.C. Lloyd-Jones, Base-catalyzed aryl-$B(OH)_2$ protodeboronation revisited: from concerted proton transfer to liberation of a transient aryl anion, J. Am. Chem. Soc. 139 (2017) 13156–13165.
[36] H.L.D. Hayes, R. Wei, M. Assante, K.J. Geogheghan, N. Jin, S. Tomasi, G. Noonan, A.G. Leach, G.C. Lloyd-Jones, Protodeboronation of (Hetero)Arylboronic esters: direct versus prehydrolytic pathways and self-/auto-catalysis, J. Am. Chem. Soc. 143 (2021) 14814–14826.
[37] W.W. Huang, H. Wang, X.L. Zhu, D.S. Yang, S.T. Yu, F.S. Liu, X.Y. Song, Highly efficient application of Mg/Al layered double oxides catalysts in the methanolysis of polycarbonate, Appl. Clay Sci. 202 (2021) 9.
[38] S. Nishimura, A. Takagaki, K. Ebitani, Characterization, synthesis and catalysis of hydrotalcite-related materials for highly efficient materials transformations, Green Chem. 15 (2013) 2026–2042.
[39] G. Hincapie, D. Lopez, A. Moreno, Infrared analysis of methanol adsorption on mixed oxides derived from Mg/Al hydrotalcite catalysts for transesterification reactions, Catal. Today 302 (2018) 277–285.
[40] Q. Zhao, S.L. Tian, L.X. Yan, Q.L. Zhang, P. Ning, Novel HCN sorbents based on layered double hydroxides: sorption mechanism and performance, J. Hazard. Mater. 285 (2015) 250–258.
[41] E. Shangguan, P.Y. Fu, S.S. Ning, C.K. Wu, J. Li, X.W. Cai, Z.H. Wang, M.Y. Wang, X.G. Li, Q.M. Li, ZnAl-layered double hydroxide nanosheets-coated ZnO@C microspheres with improved cycling performance as advanced anode materials for zinc-based rechargeable batteries, J. Power Sources 422 (2019) 145–155.
[42] Q.H. Yan, Y.S. Gao, Y.R. Li, M.A. Vasiliades, S.N. Chen, C. Zhang, R.R. Gui, Q. Wang, T.Y. Zhu, A.M. Efstathiou, Promotional effect of Ce doping in $Cu_4Al_1O_x$-LDO catalyst for low-T practical NH_3-SCR: steady-state and transient kinetics studies, Appl. Catal. B Environ. 255 (2019) 18.
[43] Y.S. Gao, Z. Zhang, J.W. Wu, X.F. Yi, A.M. Zheng, A. Umar, D. O'Hare, Q. Wang, Comprehensive investigation of CO_2 adsorption on Mg-Al-CO_3 LDH-derived mixed metal oxides, J. Mater. Chem. A 1 (2013) 12782–12790.
[44] S. Cadars, G. Layrac, C. Gérardin, M. Deschamps, J.R. Yates, D. Tichit, D. Massiot, Identification and quantification of defects in the cation ordering in Mg/Al layered double hydroxides, Chem. Mater. 23 (2011) 2821–2831.
[45] M.H. Abdellattif, M. Mokhtar, MgAl-layered double hydroxide solid base catalysts for henry reaction: a green protocol, Catalysts 8 (2018) 16.
[46] T. Montanari, M. Sisani, M. Nocchetti, R. Vivani, M.C.H. Delgado, G. Ramis, G. Busca, U. Costantino, Zinc-aluminum hydrotalcites as precursors of basic catalysts: preparation, characterization and study of the activation of methanol, Catal. Today 152 (2010) 104–109.
[47] B.H. Yan, S.Y. Zhang, M.H. Zhang, Y.K. Yu, T.H. Qin, L.P. Tang, Y. Liu, W.X. Wu, Q. Q. Mei, Green recycling of waste PET plastic monomers by banana peel extract, Chem. Eng. J. 474 (2023) 10.